Simulation of Electrical Discharge Development at Interface of Solid and Liquid Dielectrics

G.Z. Usmanov, V.V. Lopatin*, M.D. Noskov, A.A. Cheglokov

Seversk State Technological Academy, Kommunisticheskij av. 65, Seversk Tomsk reg., 636036, Russia, +7(3823)546426, E-mail: cheglok@ssti.ru

** Research Institute of High Voltages, Lenina av., 2a, 634050, Tomsk, Russia*

Abstract – The aim of present work is investigation of combined liquid-solid dielectric breakdown between needle-needle laid electrode geometry and the discovering of possible reason of the discharge channel inculcation into the solid dielectric. The volt-second characteristics of the liquid and solid dielectrics are simulated in the needle-plain electrode geometry. The breakdown occurs earlier in solid dielectric at high applied voltage steepness, but at steepness breakdown occurs preferably in liquid dielectric. The characteristics of discharge channel inculcation into the solid dielectric are obtained. It is found that the discharge inculcation efficiency into the solid dielectric rises with increase of the voltage steepness.

1. Introduction

Investigation of the discharge channel inculcation into solid dielectric in case of liquid-solid dielectric breakdown is interested both scientific and practical viewpoint due to active development of the high-voltage pulse power equipment and electrical discharge technology such as electrical grinding and drilling [1–4]. Usage of the mathematical modeling has great potential for quantitative description of the discharge development and prediction of the discharge trajectory.

Success in simulation of stochastically branched growth of discharge channels has been achieved due to development of dielectric breakdown model [5]. In this model the initiation and propagation of channels stochastically depends on the electric field. The field is calculated by solution of Laplace's equation, and the existing discharge structure has been considered as an extension of the electrode. The probability of channel extension is assumed to be proportional to a power of the local field strength. The model has been improved [6] with the introduction of a critical field strength for channel growth and constant voltage drop along the channels. However, these models are limited since they lack consideration of charge transport along the discharge channels. To overcome these limitations a self-consistent approach to modeling has been developed in papers [7–10]. According to this approach channel growth electric field variation, charge movement and change of channel conduction are considered as self-consistent and interrelated processes. In the present paper the model is further developed and used for investigation of the discharge channel propagation development in combined solid-liquid dielectric.

2. Model of discharge development

Discharge channels development is simulated with the help of a numerical discrete model created on the base of the stochastic-deterministic approach [7–10]. The discrete algorithm involves stochastic description of growth of the discharge channel and deterministic calculation of electric field by means Poisson equation, charge dynamics on the basis of Ohm law and charge conservation law and the channel conduction variation with the aid of a modified Rompe-Wiezel equation. Total equations system is presented in [10].

Solution of the numerical equations is carried out by means of explicit-implicit scheme using the physical process separation method. The discrete time steps n with the constant interval Δt are used in the model. The simulation region is covered by uniform cubic lattice of side h. The state of each lattice point *(i, j, k)* at the time step n is characterized by the variable potential φ^n_{ijk} and charge density ρ^n_{ijk}. The discharge channels structure is represented as a set of the linear elements *(i, j, k, i', j', k')* connecting centers of the adjacent lattice points *(i, j, k)* and *(i', j', k')*. The channel elements at the time step n are characterized by linear conduction $\gamma^n_{ijki'j'k'}$. The material state at each lattice point *(i, j, k)* is determined by the following values: relative permittivity ε_{ijk}, critical field E^c_{ijk}, specific conductivity σ_{ijk}, growth rate α_{ijk}, initial linear conductivity $(\gamma_0)_{ijk}$ and increase χ_{ijk} and decrease ξ_{ijk} coefficients of the linear conduction.

At each time steps an arbitrary number of lattice points can be appended to the previous discharge structure. The probability of the discharge structure element formation between the point *(i', j', k')* and the point *(i, j, k)* of the existing discharge structure is given by:

$$P^{n+1}_{ijki'j'k'} = 1 - e^{-\alpha_{i'j'k'}\left(E^n_{ijki'j'k'}\right)^2 \Delta t\, \theta\left(E^n_{ijki'j'k'} - E^c_{i'j'k'}\right)}, \quad (1)$$

where $E^n_{ijki'j'k'} = \left(\varphi^n_{i'j'k'} - \varphi^n_{ijk}\right)/h$ is electric field strength, h is the distance between points *(i, j, k)* and *(i', j', k')*. The attachment of the new points to the discharge structure occurs, if a random number R with uniform distribution within the interval [0..1) will be

less than $P^{n+1}_{i\,j\,k\,i'\,j'\,k'}$ and does not occur otherwise. The attachment probabilities for different points are statistically independent.

Distributions of electric potential and charge density at the time step *n* are calculated as:

$$\varphi^{n+1}_{i\,j\,k} = \left(\sum_{(i',j',k')\in A_{ijk}} \frac{1}{h^2}\varepsilon_{i\,j\,k\,i'\,j'\,k'}\varphi^{n+1}_{i'\,j'\,k'} + \frac{1}{\varepsilon_0}\rho^{n+1}_{i\,j\,k} \right) \Bigg/ \sum_{(i',j',k')\in A_{ijk}} \frac{1}{h^2}\varepsilon_{i\,j\,k\,i'\,j'\,k'}, \quad (2)$$

$$\rho^{n+1}_{i\,j\,k} = \rho^{n}_{i\,j\,k} + \Delta t \sum_{(i',j',k')\in A_{ijk}} \frac{1}{h^2}\sigma_{i\,j\,k\,i'\,j'\,k'}\left(\varphi^{n+1}_{i'\,j'\,k'} - \varphi^{n+1}_{i\,j\,k}\right) + \frac{\Delta t}{\Delta V} \sum_{(i',j',k')\in B_{ijk}} \gamma^{n}_{i\,j\,k\,i'\,j'\,k'}\,E^{n}_{i\,j\,k\,i'\,j'\,k'}, \quad (3)$$

$$\varepsilon_{i\,j\,k\,i'\,j'\,k'} = \frac{2\varepsilon_{i\,j\,k}\varepsilon_{i'\,j'\,k'}}{\varepsilon_{i\,j\,k}+\varepsilon_{i'\,j'\,k'}}, \quad \sigma_{i\,j\,k\,i'\,j'\,k'} = 2\frac{\sigma_{i\,j\,k}\sigma_{i'\,j'\,k'}}{\sigma_{i\,j\,k}+\sigma_{i'\,j'\,k'}},$$

where A_{ijk} is the set of neighboring points with the point *(i,j,k)* without diagonal neighbors, B_{ijk} is the set of neighboring points with the point *(i,j,k)* together with diagonal neighbors.

The linear conduction at the time step $n+1$ is given by:

$$\gamma^{n+1}_{i\,j\,k\,i'\,j'\,k'} = \gamma^{n}_{i\,j\,k\,i'\,j'\,k'} + \gamma^{n}_{i\,j\,k\,i'\,j'\,k'}\,\Delta t\left(\chi_{i'\,j'\,k'}(E^{n+1}_{i\,j\,k\,i'\,j'\,k'})^2 - \xi_{i'\,j'\,k'}\right), \quad (4)$$

The model includes five parameters, α, E_C, χ, ξ, γ_0, which, together with the form of the sample and electrodes geometry determine spatial-temporal and current characteristics of the discharge.

3. Simulation results

Simulation of the discharge development has been carried out in the needle-plane electrode geometry for liquid and solid dielectric and in the needle-needle electrode geometry for the combined liquid-solid dielectric. To determine influence of the voltage steepness on the discharge channel volt-second characteristics of the liquid and solid dielectrics breakdown have been obtained in the needle-plane electrode geometry. The choice of the simulation parameters is based on the comparison of simulation results and experimental volt-second characteristics which are presented in [2]. The model parameters related with the dielectric properties were different for solid and liquid phase (Table 1).

Table 1. Model parameters

	E_c MV/m	ε	$\alpha\cdot10^{-8}$ $m^2/V^2\cdot s$	γ_0 10^{-9} S·m	$\chi\cdot10^{-5}$ $S\cdot m^2/J$	ξ $10^7\cdot s^{-1}$
liquid	15	81	3	1,5	1	1,5
solid	25	5	20	5	3	5

The distributions of the breakdown time lags and instantaneous values of the applied voltage at the breakdown are shown in Fig. 1. The breakdown occurs preferably in solid dielectric at high applied voltage steepness (A>540 kV/μs), but at low voltage rate breakdown occurs earlier in liquid dielectric (A<540 kV/μs). The simulated voltage-time characteristics (Fig. 1) are in good agreement with the experimental data presented in [2].

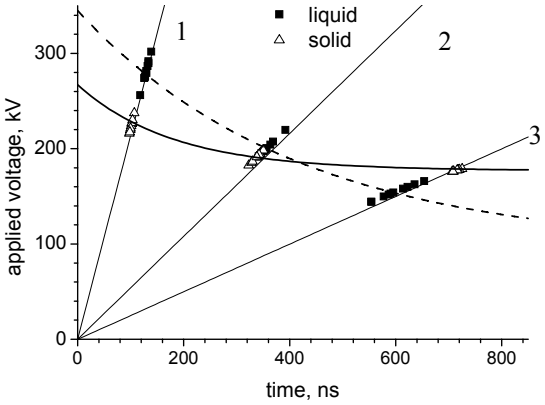

Fig. 1. Breakdown time and voltage distributions for liquid and solid dielectrics. 1 – A= 2140 kV/μs, 2 –A=540 kV/μs, 3–A = 250 kV/μs, approximations: —for solid, --- for liquid. Electrode gap d = 2 cm

This fact can be explained by the higher values of the critical field E_C for channel initiation and higher speed of channel propagation in solid dielectric in comparison with the liquid dielectric. The higher critical field in the solid dielectric leads to the later initiation of the discharge but due to higher speed of channels propagation the breakdown time of the solid dielectric less than the liquid at the higher voltage steepness (Table 2). In Table 3 the time and average speed of the discharge channels growth are shown. The growth speed is determined by growth rate coefficient α, the initial channel conduction γ_0, increase χ and decrease ξ conduction coefficients.

Table 2. Breakdown time lags

A, kV/μs	Initiation times, ns		Breakdown time, ns	
	liquid	solid	liquid	solid
250	685 ± 12	903 ± 1,5	808 ± 11	925 ± 2
540	423 ± 6,2	481 ± 2,8	522 ± 4,4	501 ± 2,6
2140	164 ± 3	180 ± 1	225 ± 1,8	197 ± 1

Table 3. Speeds of the channels growth

A, kV/μs	Growth time, ns		Speed, km/s	
	liquid	solid	liquid	solid
250	124 ± 6,8	21,5 ± 1.5	166,7 ± 10	968 ± 69
540	97 ± 4,5	19,3 ± 0.9	210 ± 9,7	1057 ± 50
2140	61 ± 2,6	17,4 ± 0,8	332 ± 13	1173 ± 57

Simulation of the discharge propagation for needle-needle electrode geometry has been carried out for the voltage steepness values close to ones used for the needle-plain geometry. Parameters describing proper-

ties of the liquid and solid dielectrics were chosen the same as in the case of the needle-plane electrode system. Electrode gap d was equal 2 cm.

At the lower pulse steepness discharge channel growth begins in the liquid dielectric due to less critical field. Channel trajectory is placed mainly along solid-liquid interface within the liquid and the inculcation into the solid dielectric is unlikely (Fig. 2) (the main discharge channel is shown in Fig. 2b by thick line).

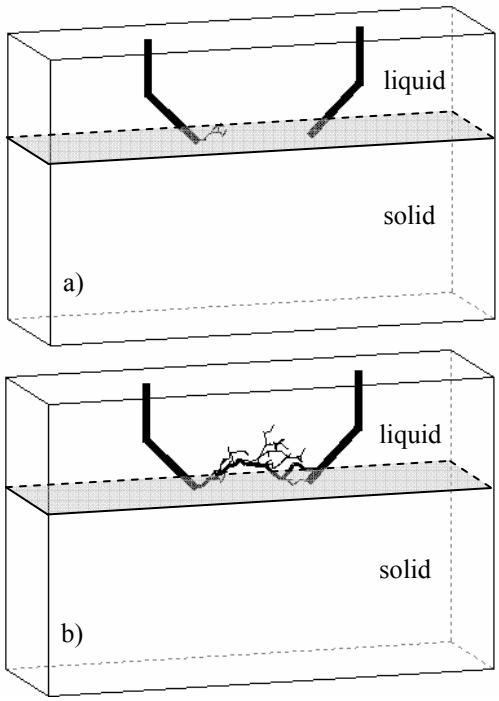

Fig. 2. Discharge structure development in combined solid-liquid dielectric at voltage rise rate A = 250 kV/μs: a) t = 700 ns, b) t = 832 ns

At the high pulse steepness inculcation of the discharge channels into the solid dielectric is more probably. Discharge starts with the formation of one or several channels from the initiating needle, when the electric field strength exceeds the critical field. Discharge channels development begins in the liquid dielectric due to smaller critical field E_C for channels growth there. Inculcation occurs when electric field strength at the channel tips exceeds the critical field for the solid dielectric. Despite the fact that growth of the discharge channels continues in the liquid dielectric, channels which propagate in the solid dielectric bridge first the discharge gap due to greater propagation speed in the solid dielectric (Fig. 3).

As a result of discharge development electrode gap bridging by main discharge channel occurs (the main discharge channel is shown in Fig. 3b by thick line) in which the pulse generator energy will be released.

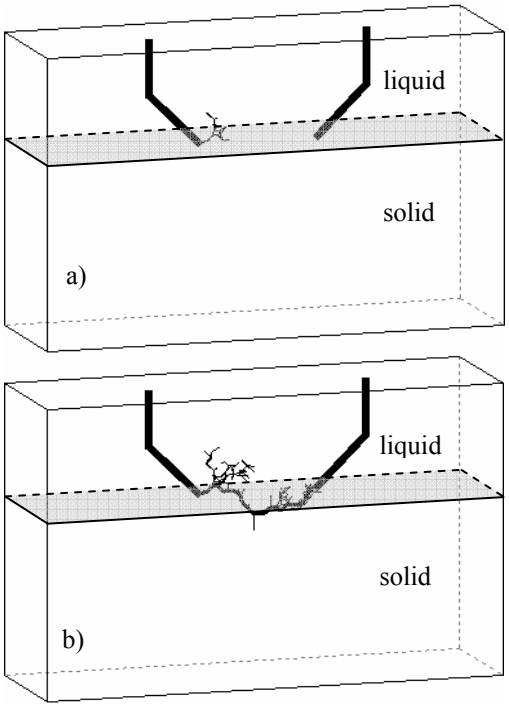

Fig. 3. Discharge structure development in combined solid-liquid dielectric at voltage rise rate A = 2140 kV/μs a) t = 200 ns, b) t = 221 ns

Efficiency of the electrical discharge destruction of solid material depends on the depth of the channel trajectory inculcation into it. For quantitative evaluation of the discharge channel inculcation in solid dielectric we used the efficiency of inculcation P, the maximal deep of inculcation h_{max} and the average deep of inculcation $<h>$.

The efficiency of inculcation is defined as:

$$P = \int_{L_M} h_l \, dl_z , \tag{5}$$

where h_1 is the distance between discharge channel segment dl and the interface layer, dl_z is the projection of the segment dl onto the interface. The integration is made over the trajectory L_M of the main discharge channel connecting the electrodes.

Maximal depth of inculcation is defined as:

$$h_{max} = \max_{L_M} h_l . \tag{6}$$

Average depth of inculcation is calculated as:

$$< h >= P / l_z , \tag{7}$$

where l_z is the length of the projection of the trajectory L_M onto the interface.

To investigate pulse steepness influence on inculcation characteristics computer experiments carried out for different values of the voltage rise. The results are presented on the Fig. 4 – Fig. 6 (an average of ten computer experiments).

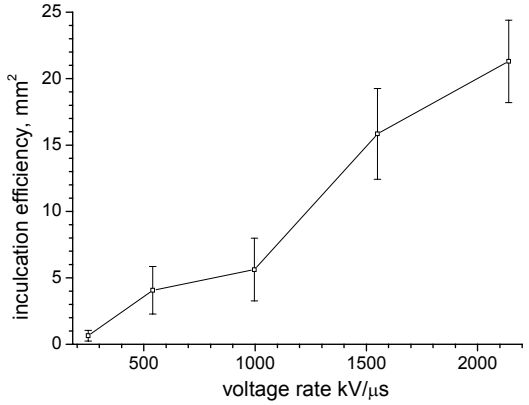

Fig. 4. Average value of inculcation efficiency with standard deviation as a function of voltage steepness

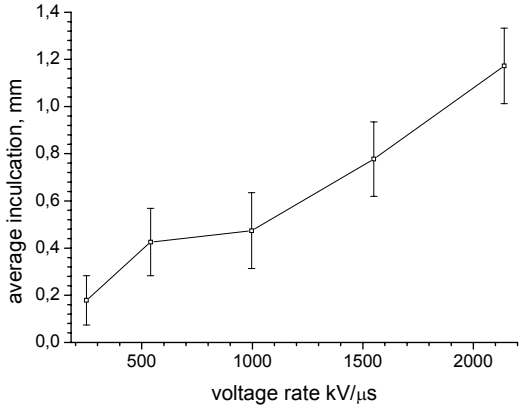

Fig. 5. Average value of mean inculcation depth with standard deviation as a function of voltage steepness

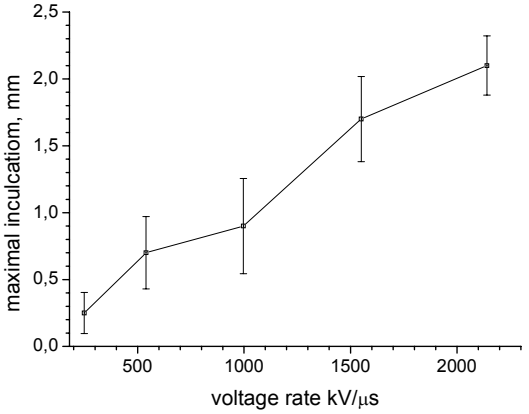

Fig. 6. Average value of maximal inculcation with standard deviation as a function of voltage steepness

Increase of the pulse steepness rise leads to the increase of all inculcation characteristics. Increase of the efficiency of the steepness inculcation into the solid with the growth of the voltage steepness can be consequence of the greater speed of discharge channels propagation and higher critical field E_C for channel growth within the solid dielectric in comparison with liquid dielectric. Thus by the stochastic-deterministic modeling it is possible to simulate effect of the discharge channel inculcation into solid dielectric which is observed when pulse steepness increases [2].

4. Conclusion

Simulated volt-second characteristics of the liquid and solid dielectrics breakdown in the needle-plane electrode system are in a good agreement with the experimental data. Analysis of the simulation results allows us to find that the greater speed of discharge channels propagation and higher critical field within the solid dielectric in comparison with liquid dielectric leads to increase of the efficiency of the discharge channels inculcation into the solid dielectric with the growth of the voltage rise rate:

The obtained results can be used for the improvement of the pulse power equipment and technology of the electrical drilling and destruction.

This work was supported by grants of RFBR №05–08–50203, and CRDF №RUE 1–1360(2)–T0–04.

References

[1] A.A. Vorobiev, G.A. Vorobiev, E.K. Zavadovska, etc *Pulse breakdown and destruction of dielectrics and rocks.*, Tomsk, TSU, 1971, 227 p. (in Russian).

[2] B.V. Semkin, A.F. Usov, V.I. Kurets *The principles of the electric impulse destruction of material*, RAS, 1995, 278 p. (in Russian).

[3] G.A. Mesyats, JTP Letters, **31,** 2005.

[4] G.A. Mesyats. *Pulsed power and electronics*. Moscow: Nauka, 2004, 704p.

[5] L. Niemeyer, L. Pietronero, H.J. Wiesmann, Phys. Rev. Lett. **52**, 1033 (1984).

[6] H.J. Wiesmann, H.R.Zeller, J. Appl. Phys. **60**, 51 1770 (1986).

[7] V.V. Lopatin, M.D. Noskov, R. Badent, K. Kist, A.J. Schwab, IEEE Trans. Diel. EI **5**, 250 (1998).

[8] M.D. Noskov, V.V. Lopatin, V.I. Kurets *in Proc. Int. Conf. on pulse power applications*, 2001, pp.F.06/1– F.06/6.

[9] Noskov M.D., Malinovski A.S., Cooke C.M., Wright K.A., Schwab A.J., J. Appl. Phys., **92**, 4926 (2002).

[10] V.V. Lopatin, M.D. Noskov, G.Z. Usmanov, A.A. Cheglokov, Izv.Vuzov "Physics", **3**, 11. (2006). (in Russian).